Arch. Metall. Mater. **69** (2024), 4, 1555-1564

DOI: https://doi.org/10.24425/amm.2024.151426

B. GASSAMA[1], B. KARAHISAR[1], N. ÖZTÜRK KÖRPE[2], M.Ö. ÖTEYAKA[3*]

CRYOGENIC TREATMENT EFFECT ON THE WEAR RESISTANCE OF AM60 MAGNESIUM ALLOY

Magnesium alloys were used as structural materials due to their low density. However, the poor wear behavior of magnesium alloys limits their use. In this study, AM60 magnesium alloy was subjected to deep cryogenic heat treatment to enhance the wear properties in dry and wet conditions with different loads. For this purpose, a deep cryogenic treatment at –196°C was applied for 48 h to the AM60 magnesium alloy. On the other hand, the wear performance of the treated sample was compared to the untreated sample using the pin-on-disc method at loads of 1 N, 2 N, and 3 N. The microstructure and wear groove were investigated using imaging techniques, while the XRD method characterized the phase modification. The results showed that the microstructures of the untreated sample drastically changed; the eutectic phase around the β phase was dissolved in the matrix, and some twins were formed after heat treatment. The XRD analysis confirmed the formation of a new β phase belonging to twins and an increase of the current β phase. Regarding hardness behavior, it increased by ~17.5% compared to the untreated sample after cryogenic treatment. In dry conditions, abrasive wear was the primary mechanism, and the wear resistance was better for the treated sample for all loads applied due to probably new phase formation. The treated sample exhibited lower wear resistance against the untreated sample, apparently due to the oxidative wear mechanism.

Keywords: Magnesium alloys; AM60; wear; cryogenic; heat treatment

1. Introduction

Magnesium, one of the lightest of all light metals, is also one of the most abundant materials in the earth's crust (the eighth most abundant material in the universe). In recent years, it has been closely studied for use as a structural material in engineering, especially in areas where lightweight is a crucial necessity [1-6]. AZ and AM series of magnesium alloys were widely used among magnesium alloys, especially AZ91 and AM60. The AM60 alloys are one of those magnesium alloys that studies are being carried on as prospects of engineering materials [7,8]. This alloy AM60 is mainly due to the good strength-to-weight ratio that the alloys display. The AM60 combines aluminum, manganese, and other alloying elements to form an alloy with good mechanical strength and ductility and is considerably more corrosion-resistant than pure magnesium [9-13]. Magnesium alloys are known for being easily corroded when exposed to corrosive environments [9,14,15] and their weak wear resistance compared to most engineering materials [1,12]. As a result, work must be done on its corrosion and wear resistance performance to be a strong prospect in engineering materials. Different studies were reported on the wear performance of AM60 at different loads and conditions [14,15]. For example, Aattthisugan et al. studied at varying loads, 10 N and 20 N, under the ambient condition at 1 ms^{-1} the wear properties of AM60 alloy [15]. They showed that the wear resistance decreased significantly by increasing the load and the distance. Zhiwen et al. coated with ion implantation and by gradient duplex Al/AlN/CrAlN/CrN/MoS2 the AM60 to enhance the wear property [14]. The AM60 alloy coated with duplex coating decreased the wear rate from 3.15×10^{-4} mm^3/N to 2.31×10^{-6} mm^3/Nm, meaning a reduction of 136 times. In another work, the AM60B magnesium alloy was coated with plasma electrolytic oxidation (PEO) to increase the wear resistance at elevated temperatures in wet conditions [16]. The PEO-coated sample exhibited a lower coefficient of friction and higher wear resistance due to the coating's porous structure and high hardness. Furthermore, they also pointed out that the wear rate increased with the increase in load and temperature.

[1] ESKIŞEHIR OSMANGAZI UNIVERSITY, INSTITUT OF SCIENCE, DEPARTMENT OF AVIATION AND TECHNOLOGY, 26040, ESKIŞEHIR, TURKEY
[2] ESKIŞEHIR OSMANGAZI UNIVERSITY, FACULTY OF ENGINEERING AND ARCHITECTURE, DEPARTMENT OF METALLURGY AND MATERIALS, 26040, ESKIŞEHIR, TURKEY
[3] ESKIŞEHIR OSMANGAZI UNIVERSITY, ESKIŞEHIR VOCATIONAL SCHOOL, DEPARTMENT OF MECHATRONIC, 26110, ESKIŞEHIR, TURKEY

* Corresponding author: moteyaka@ogu.edu.tr

On the other hand, the wear performance of the as-cast AM60 alloy subjected to friction stir processing (FSP) was examined by Iwaszko et al. [17]. A load of 20 N was applied on the surface of the stirred zone using the pin-on-disc method and thermomechanically affected zone in dry conditions. A decrease in friction coefficient for the FSP sample compared to the untreated was found.

Different elements were added to the alloy to enhance the wear resistance of AM60. For example, Chenghao et al. investigated the effect of rare mixed earth; (RE) La and Ce on the wear performance of AM60. They found that the addition of RE decreased the coefficient of friction and specific wear rate due to refining the grains of the α phase and $Mg_{17}Al_{12}$ phase [11]. Yong and Li [12] studied the addition of 1 wt.% silicon to the mechanical properties of AM60. The wear weight loss of the without silicon AM60 alloy was superior compared to the silicon-added AM60. Moreover, it was more pronounced for the load 60-80 N; by contrast, it was equal at low loads between 20-30 N. The better wear performance at high loads was due to the formation of Mg_2Si, which has a higher hardness than the matrix.

Recently, cryogenic heat treatment was investigated to enhance the wear resistance of light metals. Cryogenic heat treatment is a method that has been previously used to improve both the wear and corrosion resistance of certain materials in the engineering world [18-20]. This heat treatment works well with steel because it increases the mechanical properties by dissolving more residual austenite phases [21-24]. Currently, it begins to investigate the effect of cryogenic treatment on light metals such as Ti [25], Al [26,27], and Mg [20]. This heat treatment may enhance the wear behavior of AM60 and open a new area of research. Herein, we investigated the effect of deep cryogenic treatment on the wear resistance of AM60 magnesium alloy in dry and wet conditions with different wear loads.

2. Materials and methods

2.1. Sample preparation and heat treatment

The as-cast AM60 alloys used were obtained from the Firm Varzone Ltd. in the dimension of 300×200×300 mm and cut into small cubes of 10×10×20 mm^3. The chemical composition of the material was mainly composed of aluminum (6.26%), manganese (0.29%), zinc (0.1%), and balance with magnesium. The samples were then labeled as untreated and treated, and one labeled treated was taken to be cryogenically treated whiles the labeled "untreated" waited. The labeled "treated" sample was placed in a room-temperature box. The temperature in the box was gradually reduced at a velocity of 5°C/min to the desired temperature of –196°C. The temperature at the box was maintained at –196°C for a period of 48 h whiles that sample was in the box, allowing the sample cryogenic exposure for 48 h, thus rendering it cryogenic treated, after which the temperature in the box was gradually regulated back to room temperature at a velocity of 5°C/min.

2.2. Wear test and hardness measurement

The samples under investigation were placed in a model CSM Tribometer, and the pin-on-disc method was applied. The tribometer was set at a rotational motion with a constant velocity of 3 m/s. A wear distance of 10 m was applied for all the samples that underwent the test. Loads of 1 N, 3 N, and 5 N were exerted on the steel ball (hardened-DIN 5401) at different stages of the investigation. The test was conducted in a dry condition (in the open air) and wet condition (in a solution of 0.9 wt.% NaCl). After the samples were done covering the 10 m distance set, they were removed and put under an optic microscope to take images of the surface of the samples and then taken under a profilometer to measure the wear area of the samples. The calculation of wear area and dx (wear track width) was presented in a previous study [28]. The experiments were repeated at least three times. The calculation of specific wear rate (W_{sp}) was presented in Eq. (1), where ΔV, F, and L were the total volume wear, the average load, and the total sliding distance, respectively.

$$W_s = \frac{\Delta V}{F.L} \tag{1}$$

The hardness of the samples was also investigated using a micro-hardness tester by applying a load of 5 kg/f for 10 s. An average of 10 measurements were taken an account.

2.2. Sample characterization

The surface with 10×10 mm ground with 800 and 1200 SiC grinding papers and cleaned with alcohol. The untreated and treated samples were polished with a 1 μm diamond solution napless for a mirror-like appearance. They were etched with 2% Nital for 5 s and placed under an optic microscope to take their images at the magnifications of ×1000. Furthermore, a deeper analysis was performed to see the modification after cryogenic heat treatment using scanning electron microscopy (SEM). A semi-quantitative analysis was performed to find the elements scattered in the microstructure using energy dispersive spectroscopy (EDS). The effect of heat treatment on AM60 alloy has been revealed as a result of kinetic calculations by determining the transformation temperatures using Pryis Diamand Perkin Elmer TG / DTA data. The heating process was carried out from room temperature to 700°C at a rate of 20°C/min. Argon gas passage was provided with a 100 ml/min flow rate to prevent oxidation of the samples. In addition, an X-ray diffractometer (XRD) – Panalytical EMPYREAN was carried out to determine the new phase formation after cryogenic treatment. The XRD pattern was taken in the range of 0°-90° at a speed of 5°/s.

3. Results and discussion

3.1. Microstructure and phase evaluation

The microstructure of the untreated and cryogenic treated (CT) AM60 magnesium alloys is given in Fig. 1. At first glance, we can state that the cryogenic heat treatment significantly affected the microstructure. It is well known that untreated AM60 had a dendritic structure with eutectic and β phases distributed in its microstructure [29,30]. The findings in Fig. 1a) fitting with the literature. After heat treatment, the eutectic phase around the β phase disappeared, and twin deformation was observed on the treated microstructure (Fig. 1b)). Twinning can also be observed on AM30 magnesium alloy containing lower aluminum content [31]. Twinning, which is seen to be a factor in hindering wear in these samples, can also be observed in the treated samples (Fig. 1b)), whiles no twinning would be seen with the untreated samples.

A similar observation was seen by SEM images presented in Fig. 2. It was spotted that the eutectic phase was adjacent to the β phase for untreated samples, while the eutectic phase was disassociated from the β phase for treated samples. Researchers have observed that slight twins can help improve the wear resistance of a material; it has been shown that increased twinning can decrease wear resistance in the studied material [32]. A study done on magnesium alloys indicated that the twinning in the materials caused the hardening of the materials, thus positively influencing the material's wear resistance [33]. EDS analysis was performed to understand the element distribution in the microstructure of untreated and treated AM60 (Fig. 2 and TABLE 1). In Fig. 2a), points 1, 2, and 3 for untreated AM60 match to Mg (α), $Mg_{17}Al_{12}$ (β), and eutectic ($\alpha + \beta$) phases, respectively. While points 1, 2, and 3 for treated AM60 pairing to a twin, β, and α phase, respectively (Fig. 2b)).

TABLE 1

EDS analysis of the SEM images is presented in Fig. 2

Sample	Point	Mg	Al	Mn	Zn
Untreated	1	95.09	4.60	0.12	0.19
	2	73.59	26.10	0.08	0.23
	3	91.51	8.34	0.08	0.07
Treated	1	95.12	4.65	0.11	0.12
	2	79.62	20.13	0.10	0.15
	3	91.88	7.98	0.09	0.05

The formation of a new phase after cryogenic treatment was elucidated in Fig. 3. As observed, the XRD pattern of untreated

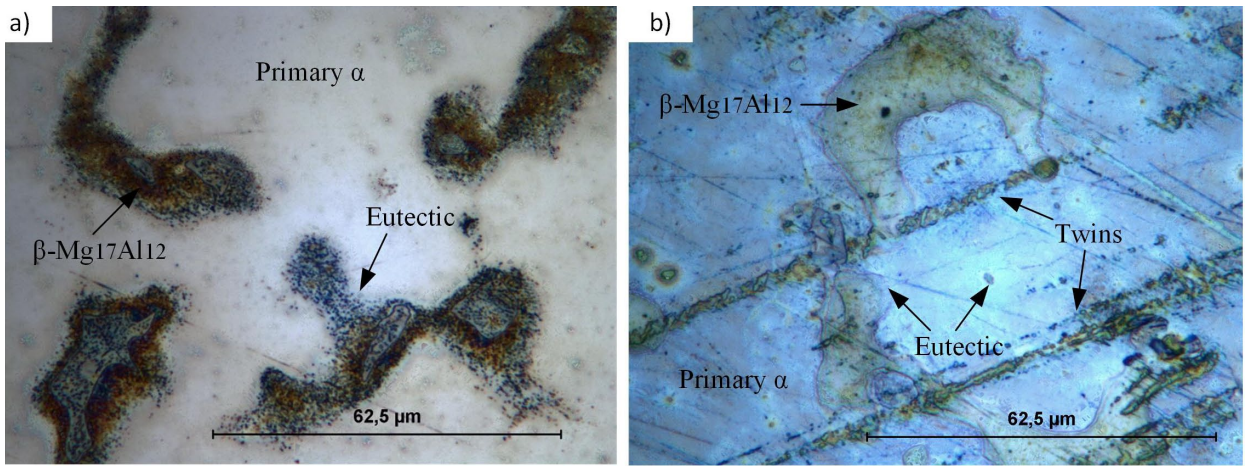

Fig. 1. The microstructure of untreated and treated AM60; a) untreated AM60 (×1000), b) treated AM60 (×1000)

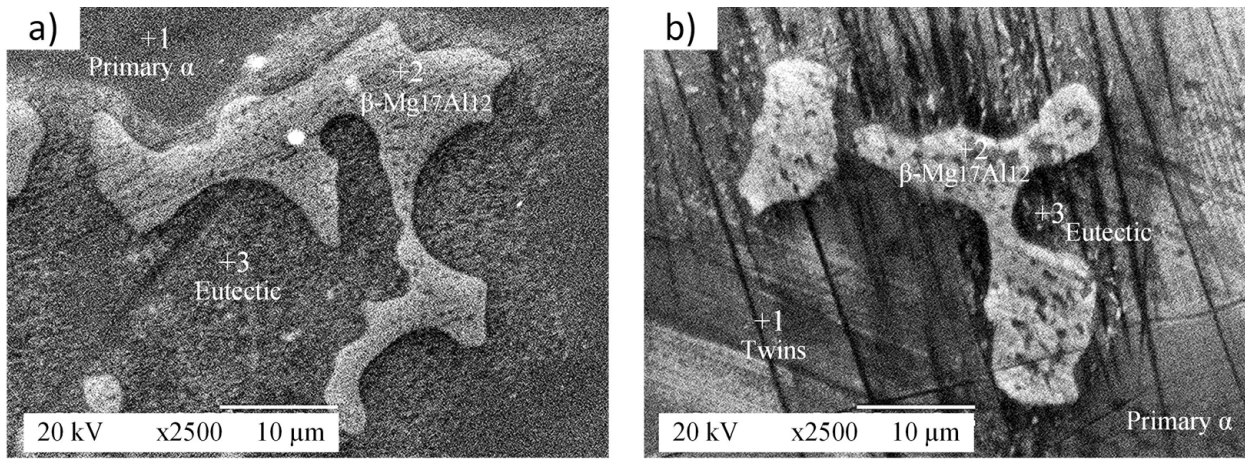

Fig. 2. SEM-EDS images of untreated and treated AM60 (×2500); a) untreated b) treated

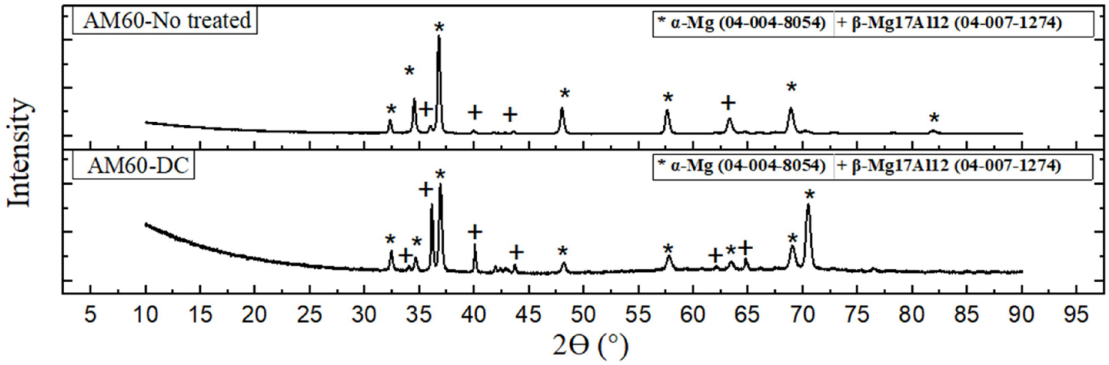

Fig. 3. XRD pattern of untreated and treated AM60 alloy

AM60 had α-Mg and β-$Mg_{17}Al_{12}$ intermetallic phases, which was no surprise. The main peak of α-Mg was located at 37°, 34°, 32°, 48°, 57°, and 68° while the β phase was situated at 36°, 40°, and 44°. These phases were also detected by different authors [30,34]. Regarding the treated AM60 XRD pattern, it is evident that after cryogenic treatment, the microstructure altered; the treatment increased the intensity of the β phase located at 36°, 40°, and 44°. Besides, new β phases were observed at 33°, 62°, and 65°. At the same time, a higher peak labeled to the α phase was found at 71°, and some α peaks decreased. It can be stated here that the heat treatment had a significant positive influence on the modification of the microstructure; the β phase was more prominent than the α phase due to the precipitation of the β phase in the α phase.

According to the Mg-Al equilibrium diagram [35], the melting begins in the region where the solubility limit is exceeded in the eutectic ($Mg_{17}Al_{12}$) structure with a melting temperature of around 437°C. In the present study, approximately the same peak temperature and enthalpy values were obtained in the 425-445°C peaks for both cases in DTA analyses. The dissolution of the $Mg_{17}Al_{12}$ eutectic and Al in the Mg matrix is in question (Fig. 4a)).

The heat-treated sample has a higher enthalpy value for this reaction than the endothermic peak when Mg primary crystals begin to melt. It is thought that the anomaly seen in the DTA curves of the treated sample before the second peak, which is different from the literature, is caused by the shrinkage pores (distortions) in this sample. Again, melting started before (593°C) in the heat-treated sample and caused a higher enthalpy value. Otherwise, the peak obtained by melting for the untreated sample is compatible with the literature (608°C) (Fig. 4b)) [36].

3.2. Wear behavior analysis

The measured hardness of the untreated sample was 57 HV; after cryogenic heat treatment, an increase of ~17.5% was observed. This hardness enhancement was probably due to the precipitation of the β phase, the distribution of the eutectic phase in the Mg, and twinning formation. Oršulová and Palček showed that precipitation on AZ91 alloys increased their hardness from 54 to 71 HBW 2.5/62.5 [37]. The data collected from the investigation showing the wear area of the untreated and treated sample under loads of 1 N, 3N, and 5N in a dry condition was presented in Fig. 5. Comparing the wear areas of the two rival samples under the 1 N load, the untreated sample has a wear area of 2230 μm^2 and dx = 330 μm while the treated sample showed a wear area of 1700 μm^2 and dx = 300 μm. The untreated sample showed ~31.2% more worn area than the treated sample. At the 3 N load, the untreated sample recorded a wear area of 5960 μm^2 and dx = 540 μm while the treated sample had a wear area of 4560 μm^2 and dx = 450 μm, the untreated sample having 1400 μm^2 more wear area than the treated sample. When the load on the samples was adjusted to 5 N, the untreated

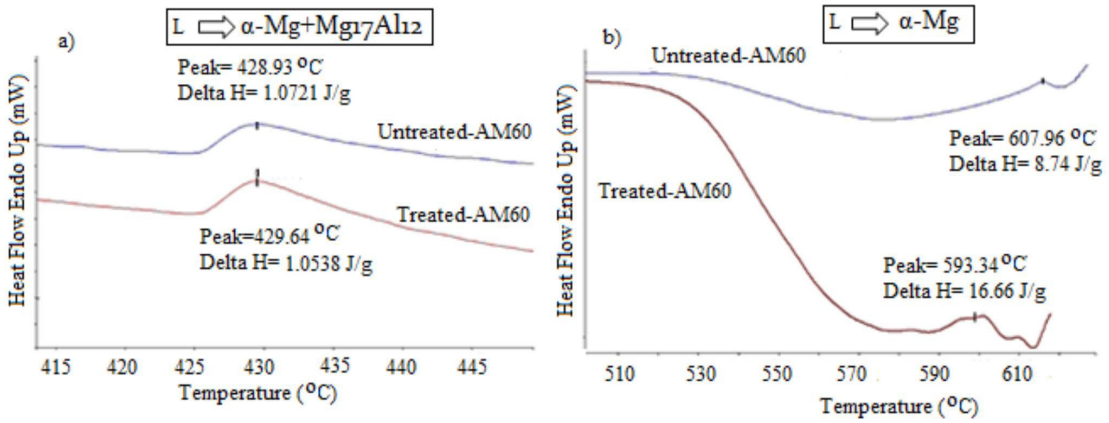

Fig. 4. TG/DTA analysis of the untreated and treated AM60 magnesium alloys; a) 415°C-450°C b) 500°C-610°C

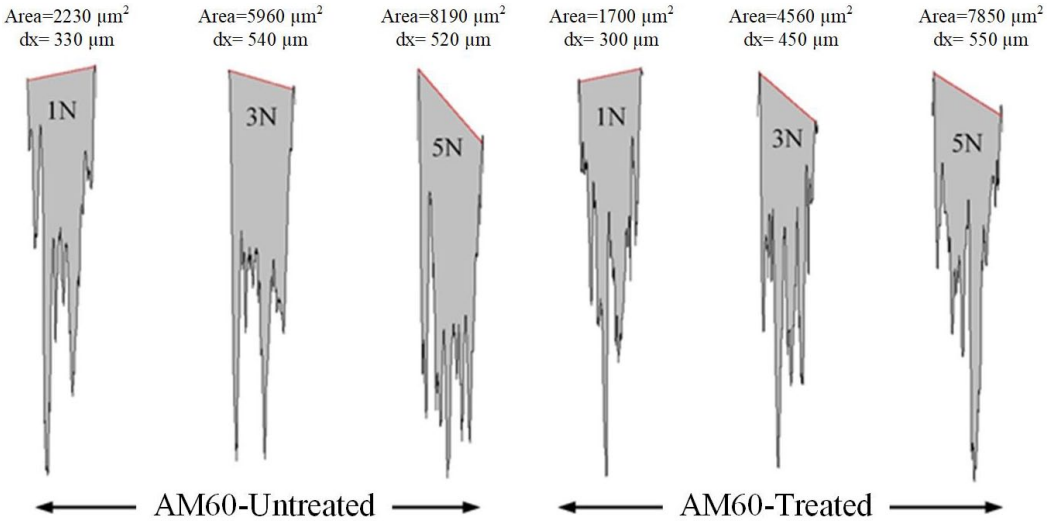

Fig. 5. Wear area and a track width of untreated and treated in the dry condition

sample displayed a wear area of 8190 µm^2 and dx = 520 µm. In contrast, the treated sample exhibited a wear area of 7850 µm^2 and dx = 550 µm, a difference in wear area of 340 µm^2 that the untreated sample has more than the treated sample. We have seen that the treated sample had a lower wear area over the untreated sample in a dry condition, meaning better wear resistance performance for all load categories.

The wear area of the untreated and treated sample under loads of 1 N, 3 N, and 5 N in a wet condition was presented in Fig. 6. When the 1 N load was exected on the steel ball that took a rotational motion on the samples, a wear area of 2598 µm^2 and dx = 420 µm was registered for the untreated sample. While the treated sample registered a wear area of 3956 µm^2 and dx = 470 µm, a difference in the area of 1358 µm^2 that the treated sample has more than the untreated sample (Fig. 6). When the 3 N load was exerted on both samples, wear area values of 6200 µm^2 dx = 560 µm and 6278 µm^2 dx = 550 µm were obtained for the untreated and treated samples, respectively, a wear area difference of 78 µm^2 that the treated sample has over the untreated sample. With the load adjusted to the 5 N load, the sample provided wear area values of 5694 µm^2 dx = 570 µm and 6513 µm^2 dx = 670 µm for the untreated and treated samples, respectively, a difference of 819 µm^2 that the treated sample has over the untreated sample. It can be observed that the values of the wear area of the sample when loads from 1 N, 3 N, and 5 N were placed on the samples under test in the wet condition. The untreated sample shows a better wear resistance performance based on the wear area of the sample. It can be stated here that the treated sample shows a greater degree of wear resistance in the dry condition compared to the wet condition.

The data comparison between the untreated and treated sample in the 1 N load category revealed that the wear rates comparison between the untreated and the treated sample in the experiment have a difference of approximately 0.8×10^{-3} mm^3/Nm. The untreated sample was seen to have the higher wear rate of the two samples being compared (Fig. 7). As the load was shifted to the 3 N category, the untreated sample was again seen to have a higher wear rate by approximately 0.7×10^{-3} mm^3/Nm when compared to the treated sample in the experiment. When the load of 5 N was exerted on the samples, the difference was approximately 0.15×10^{-3} mm^3/Nm, still in favor of the treated sample in the context of better wear resistance performance. But

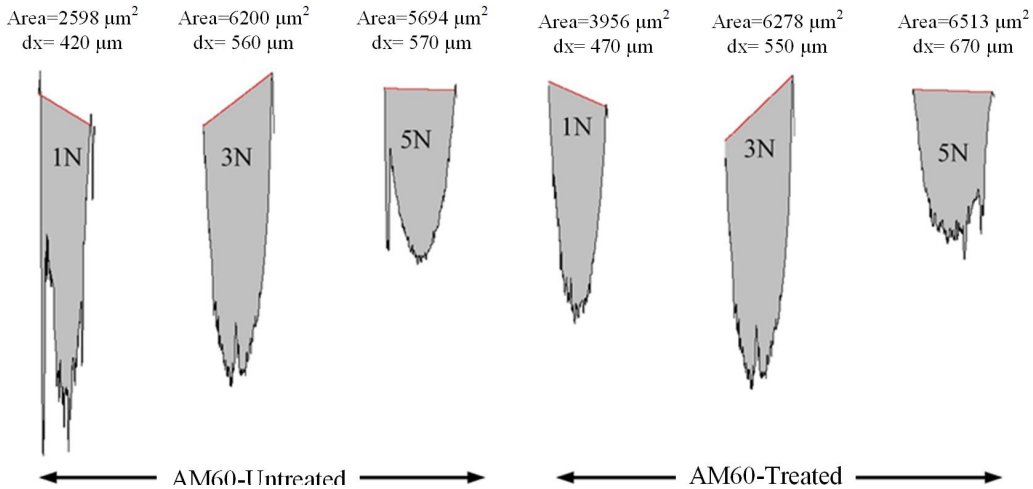

Fig. 6. Wear area and a track width of untreated and treated in the wet condition

with a much smaller difference compared to the previous weight categories. Previously, it was reported that the wear rate at low loads was higher for AM60 in dry conditions, and it decreased with the increase of the loads [38]. Overall, it can be stated here that the treated sample had a much bigger edge over the untreated sample when the load exerted on the samples was the smallest. That difference shrinks as the load increases to the middle load used in this experiment and finally gets even smaller with the higher load. It is seen that the effectiveness of the cryogenic treatment of the samples was more conspicuous in the lower loads of the experiment.

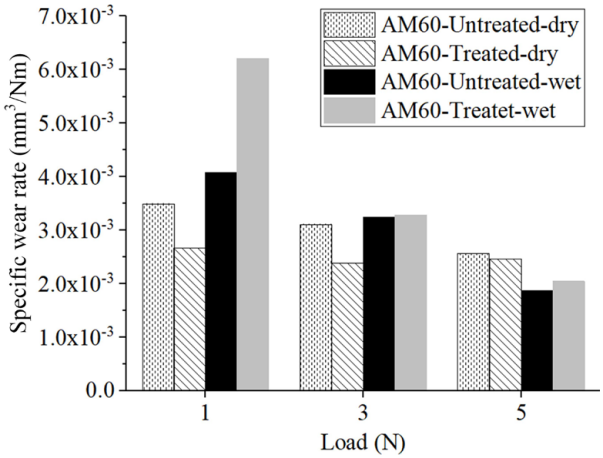

Fig. 7. The specific wear rate of untreated and treated AM60 in dry and wet conditions

Regarding the COF behavior at dry conditions, the untreated sample is seen to have an almost steady value from the beginning of the test towards the 10 m distance that the test was conducted and showed values around 0.34 μ. In contrast, the treated sample started the test around a COF value of 0.33 μ, but those values quickly rose to 0.58 μ within the first 0.5 m of the test and remained somewhat constant in that value for the rest of the 10 m of the test (Fig. 8).

When a 3 N load was put on the samples, it was seen that the untreated sample finished with an average of 0.32 μ. However, the treated sample started at a slightly lower COF value, around 0.26 μ. Still, the value quickly increased to around 0.46 μ, where the value would remain somewhat constant until around the 8 m in the test, where they dropped to 0.41 μ for the rest of the 10 m distance; the average was 0.42 μ. The 5 N load category showed average values of 0.27 μ and 0.54 μ for untreated and treated samples, respectively. The overall results showed that the untreated sample under the 5 N load had the lowest COF value for the whole test, and the treated sample under the 5 N load had the highest COF value for the whole test. Comparing the results with the literature, it registered a COF of 0.38 after a 10 N load with a sliding speed of 1 m/s [38]. In addition, the COF decreased with the increment of loads, reaching the lowest of 0.25 with 250 N. The wear track of the untreated and cryogenic treated samples that were tested in a dry condition was presented in Fig. 9. At first glance, it can be seen that wear grooves were evident, and some voids having a size of 10-30 μm were observed at the worn area for both samples.

The wear width for the treated and untreated samples when a load of 1 N was exerted on the ball was 324.4 μm and 302.3 μm, respectively, with the treated sample having 22.1 μm less wear track width. When the load of 3 N was used in the experiment, track widths of 363.6 μm and 328.8 μm were recorded for the untreated and treated samples, respectively, with the treated sample showing a 34.8 μm less wear track width than the untreated sample. And finally, when the samples were subjected to the 5 N load, the values of 494.9 μm and 447.5 μm were registered as the wear track width for the untreated and treated samples, respectively. The treated sample shows a 50.4 μm less wear track width than the rival sample. It should be noted that increasing the load induces broader and deeper grooves for both samples. The findings also show that for all the load categories from 1 N, 3 N, and 5 N, the treated sample has consistently shown better values regarding the width of their wear track in the context of good wear resistance. The primary wear behavior of AM60 magnesium alloy in a dry medium was plastic deformation, adhesion, oxidation, abrasion, and delamination [38,39]. Taltavull et al. [38] also spotted that the oxidation wear mechanism was controlled at lower loads and velocities. The wear mechanism of the studied samples can be deduced from Fig. 9; abrasive grooves and oxide formation was the primary wear mechanism for both samples.

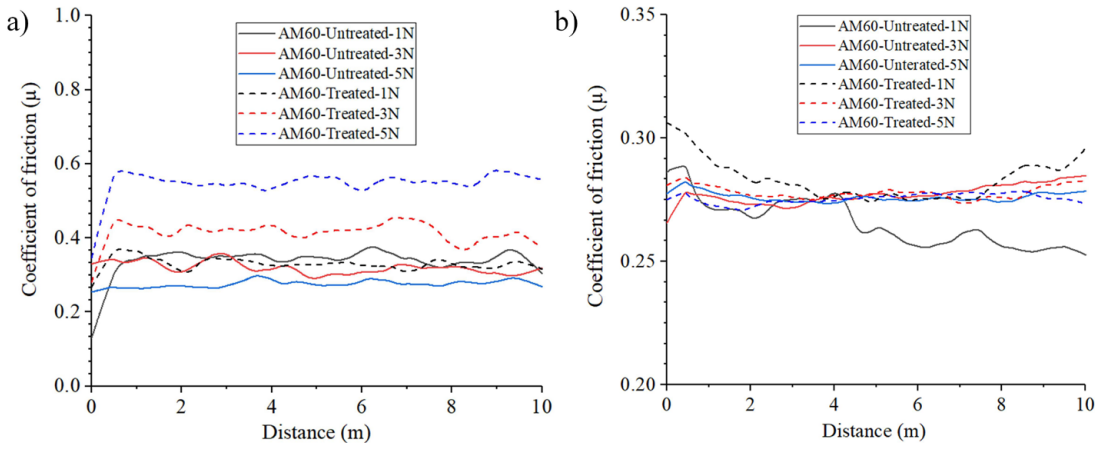

Fig. 8. Coefficient of friction behavior of untreated and treated AM60; a) dry and b) wet condition

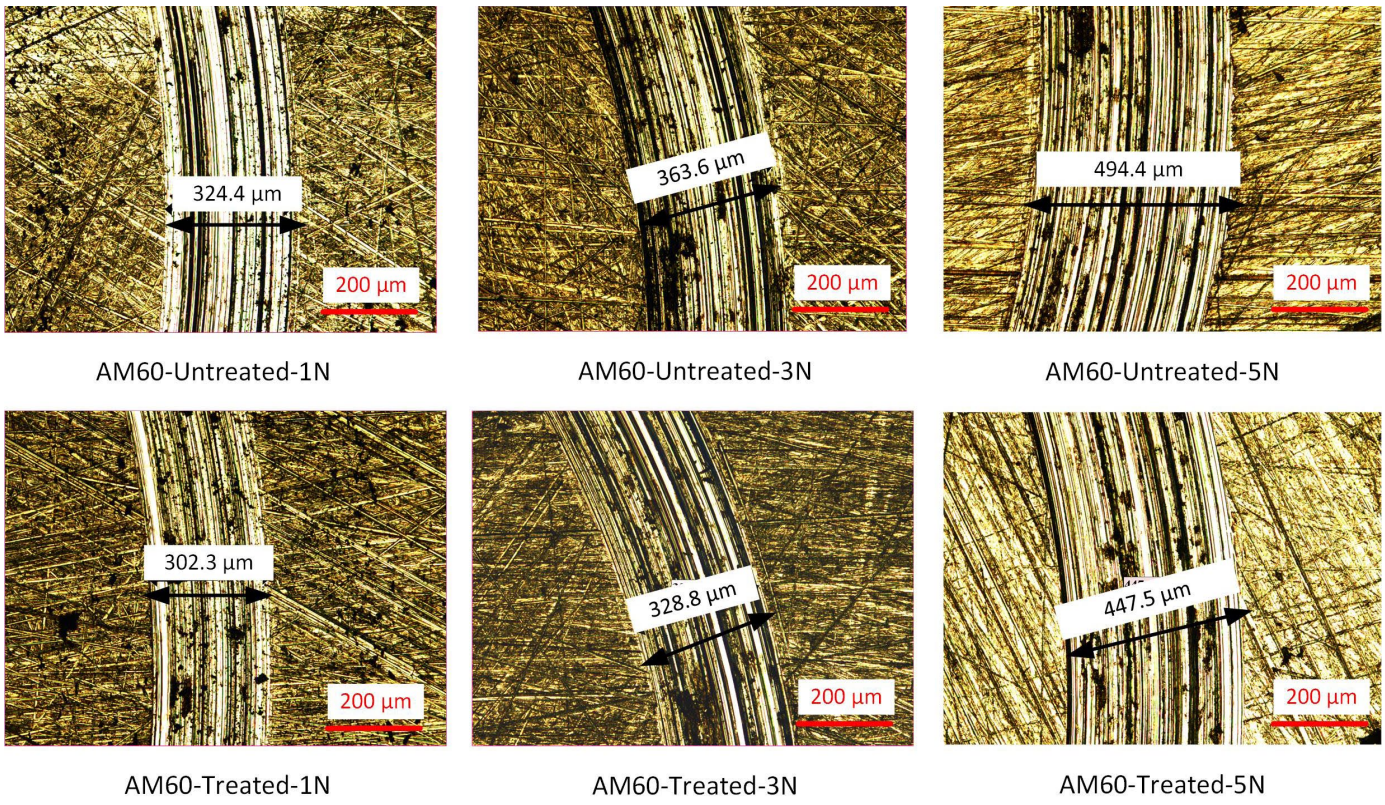

Fig. 9. Untreated and treated AM60 wear tracks in dry condition

Regarding the performance of samples in 0.9 wt.% NaCl solution; the experimental values showed that the untreated sample had a wear rate of approximately 2.1×10^{-3} mm^3/Nm less than the wear rate values exhibited by the treated sample in the wet condition (Fig. 7). As the load was increased to 3 N, the two samples were seen to have almost the same wear rate values, with the untreated sample showing a slight edge of approximately 0.5×10^{-3} mm^3/Nm over the treated sample in terms of less wear rate. When the load was higher (5N), the results showed that the untreated sample at this time had approximately 2.0×10^{-3} mm^3/Nm less than the value produced by the treated sample in the wet condition. These values show that at the lowest load applied, the wear rate for both samples was superior compared to dry condition findings. This high specific wear rate can be explained by the corrosive fluid which attacks the metal surface and form oxide debris.

On the other hand, the specific wear rate decreased when applying a 3 N load; the value came nearer to the untreated sample in dry conditions. Thus, the wear rate was the lowest at the highest load compared to dry conditions for both samples. Here, it should be noted that the corrosive environment acted as a lubricant after the 3 N load. On the other hand, the COF behavior of untreated and treated AM60 alloy was tested in a wet condition (Fig. 8). At the 1 N load, the untreated sample was seen to have started the experiment with the second-highest COF values. But the value dropped around 0.5 m of the 10 m; to be within the samples that exhibit the lower value, then 4 m in the test, it even dropped further to separate itself from the sample with the lowest COF value, an average of 0.25 µ. The study of Guo et al. on AM60 found 0.21 µ in lubrication condition after 10 N of the load was applied using a steel ball [16].

Demirci et al. reported 0.4 µ for the rival magnesium alloy AZ91 after applying a 2 N load in 3.5 wt.% NaCl [40]. However, the treated sample recorded a COF value of around 0.28 µ, which stands out as the high COF recorded amongst all the samples within the test to start the test. The value dropped around 4 minutes in the test to the level of the other samples but eventually went up again to end the test as the sample with the highest COF value recorded. All the other samples in the test recorded average COF values of 0.27 µ that were not far apart except for the sample with the 1 N load. The COF values in this wet condition could be much lower than those with the samples in the dry condition. This significant difference could be attributed to the lubricating effects of the test's condition. This difference could be the exact reason for the less wear experienced by the sample in the wet condition compared to the dry ones. The behavior shown by the sample at the 1 N load (treated and untreated) at the wet condition is the same behavior shown by samples bearing the 5 N load in the dry condition. The analysis of wear tracks after wet sliding in Fig. 10 suggests more oxide debris on the wear groove with fewer sliding traces for both samples. The adhesion and abrasion wear mechanism was seen, and the adhesion wear mechanism was more prominent. On the other hand, magnesium alloy is well documented to be susceptible to local corrosion, especially pitting corrosion in a chloride environment [41-43].

To this, localized corrosion was observed inside and outside of the worn surface of untreated and treated AM60

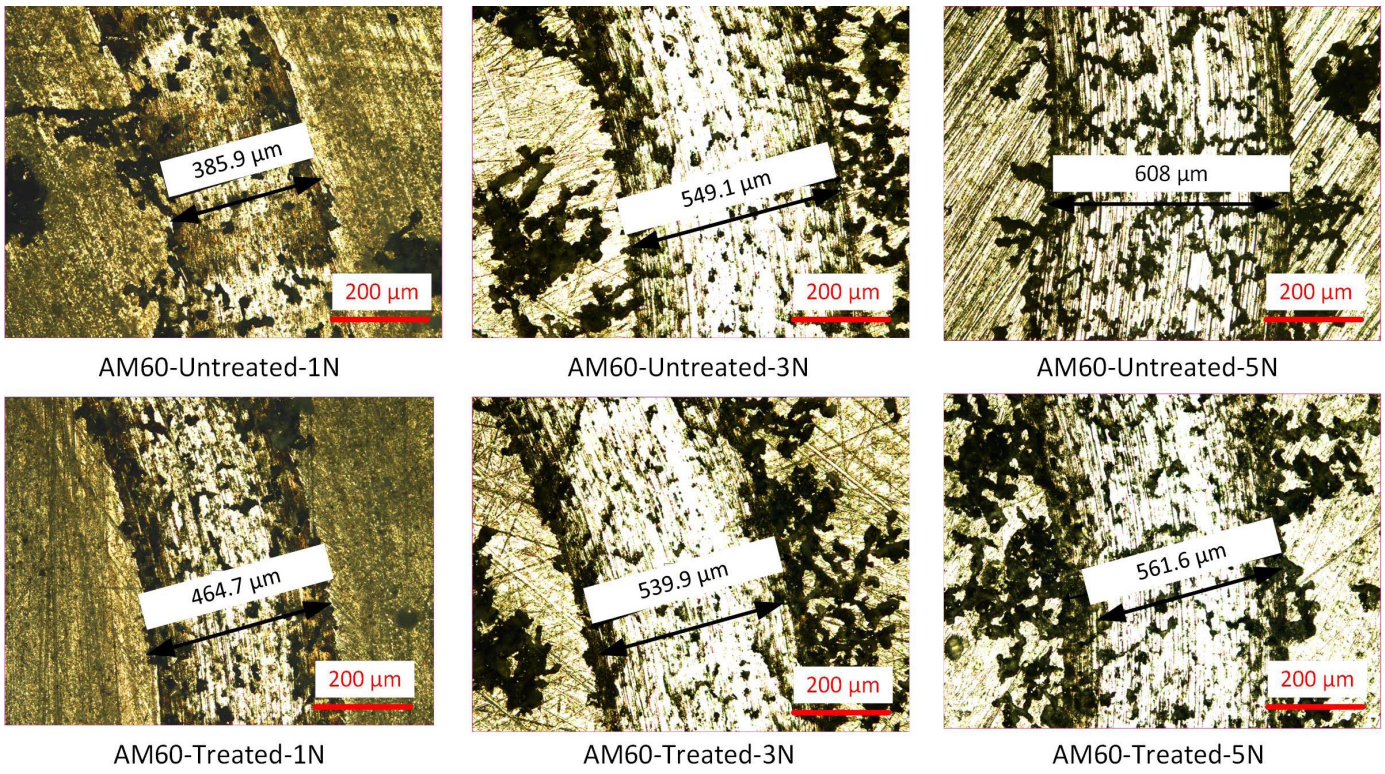

Fig. 10. Untreated and treated AM60 wear tracks in wet condition

magnesium alloy (Fig. 10). In the wet condition, the 1 N load was exerted on the steel ball as the experiment was carried on. The wear track width for the untreated and treated samples in this wet condition was 385.9 µm and 464.7 µm, respectively, with the untreated sample showing a 78.8 µm narrower wear track width (Fig. 10). When the samples were exposed to the 3 N load, the untreated and treated samples showed wear track width values of 549.1 µm and 539.9 µm, respectively, with the treated sample producing a 9.2 µm narrower wear track width than the untreated sample. As the load was increased to 5 N, their wear track width values were 608 µm and 561 µm for the untreated and treated samples, respectively, with the treated sample showing a 47 µm narrower wear track width. From the values that the samples being compared showed, the untreated sample produced better wear resistance for the lowest load category. However, as the load increased, the treated sample gradually showed better wear resistance performance. Similarly to dry condition, increasing the applied load makes the grooves broader and more profound in wet conditions. The wear on these samples tested in the wet condition is also more prolific than those conducted in the dry condition; this is primarily due to the chemical interaction between the sample and the wet condition, leading to corrosion wear.

4. Conclusions

The cryogenic treatment drastically modified the microstructure of AM60; dissolution of the β phase was more pronounced, eutectic was dispersed in the matrix, and twinning formation was observed in the microstructure. The wear resistance of cryogenically treated AM60 was addicted to the wear condition. The COF of the treated sample was higher in the dry condition than in the untreated sample. Unlike, the COF in the wet condition was lower compared dry condition for all samples. The wear rate of the cryogenically treated sample was improved in the dry condition compared to untreated AM60 due to possibly twinning formation and hardness enhancement. In adverse, the treated sample showed a worse wear resistance in the wet condition because of the less resistance of the microstructure against corrosive solution with oxide debris. The primary wear mechanism was abrasive for the dry condition, while oxidative wear was seen in the wet condition.

Acknowledgements

This study is supported by Eskişehir Osmangazi University, Scientific Research Projects Coordination Unit. Project Number: FYL-2021-2156

REFERENCES

[1] D.S. Mehta, S.H. Masood, W.Q. Song, Investigation of wear properties of magnesium and aluminum alloys for automotive applications. Journal of Materials Processing Technology **155-156**, 1526-1531 (2004).

[2] S. You, Y. Huang, K.U. Kainer, N. Hort, Recent research and developments on wrought magnesium alloys. J. Magnes. Alloy **5**, 239-253 (2017).

[3] R.D. Klassen, P.R. Roberge, A.M. Lafront, M.Ö. Öteyaka, E. Ghali, Magnesium: Proceedings of the 6th International Conference Magnesium Alloys and Their Applications. In: K.U. Kainer (Ed.) Magnesium, Wiley-VCH Verlag GmbH & Co. KGaA, p. 655-660 (2003).

[4] H. Zengin, Y. Turen, L. Elen, A Comparative Study on Microstructure, Mechanical and Tribological Properties of A4, AE41, AS41 and AJ41 Magnesium Alloys. Journal of Materials Engineering and Performance **28**, 4647-4657 (2019).

[5] C. Liang, Y.B. Wang, M.L. Yin, X.X. Lv, J. An, A Novel Method of Evaluating the Mild to Severe Wear Transition Loads for Magnesium Alloys. Journal of Materials Engineering and Performance **24**, 1406-1416 (2015).

[6] Z. Yang, J. Kang, D.S. Wilkinson, The Effect of Porosity on Fatigue of Die Cast AM60. Metallurgical and Materials Transactions A **47**, 3464-3472 (2016).

[7] Z. Chen, J. Huang, R.F. Decker, S.E. Lebeau, L.R. Walker, O.B. Cavin, T.R. Watkins, C.J. Boehlert, The Effect of Thermomechanical Processing on the Tensile, Fatigue, and Creep Behavior of Magnesium Alloy AM60. Metallurgical and Materials Transactions A **42**, 1386-1399 (2011).

[8] L.H. Rettberg, J.B. Jordon, M.F. Horstemeyer, J.W. Jones, Low-Cycle Fatigue Behavior of Die-Cast Mg Alloys AZ91 and AM60. Metallurgical and Materials Transactions A **43**, 2260-2274 (2012).

[9] P. Jia, M. Wu, J. Zhang, X. Hu, X. Teng, D. Zhao, T. Wei, D. Dong, Q. Liu, Y. Wang, Effects of Mg–Zn–Y quasicrystal addition on the microstructures, mechanical performances and corrosion behaviors of as-cast AM60 magnesium alloy. Materials Research Express **5**, 106512 (2018).

[10] B. Akyüz, Wear and machinability of AM series magnesium alloys. Mater. Test **61**, 49-55 (2019).

[11] L. Chenghao, W. Shusen, H. Naibao, Z. Zhihong, Z. Shuchun, R. Jing, Effects of Lanthanum and Cerium Mixed Rare Earth Metal on Abrasion and Corrosion Resistance of AM60 Magnesium Alloy. Rare Metal Materials and Engineering **44**, 521-526 (2015).

[12] H. Yong, R. Li, Effects of silicon on mechanical properties of AM60 magnesium alloy. China Foundry **9**, 244-247 (2012).

[13] Z.L. Liu, Y. Liu, X.Q. Liu, M.M. Wang, Effect of Minor Zn Additions on the Mechanical and Corrosion Properties of Solution-Treated AM60-2%RE Magnesium Alloy. Journal of Materials Engineering and Performance **25**, 2855-2865 (2016).

[14] Z. Xie, Z. Luo, Q. Yang, T. Chen, S. Tan, Y. Wang, Y. Luo, Improving anti-wear and anti-corrosion properties of AM60 magnesium alloy by ion implantation and Al/AlN/CrAlN/CrN/MoS2 gradient duplex coating. Vacuum **101**, 171-176 (2014).

[15] A. I, S. Kumar, A. Rose, S.J. Devaraj, Wear behaviour of am60 magnesium alloy with different load and sliding distance. International Journal of Mechanical Engineering and Technology **8**, 130-134 (2017).

[16] J. Guo, L. Wang, J. Liang, Q. Xue, F. Yan, Tribological behavior of plasma electrolytic oxidation coating on magnesium alloy with oil lubrication at elevated temperatures. Journal of Alloys and Compounds **481**, 903-909 (2009).

[17] J. Iwaszko, K. Kudla, K. Fila, M. Strzelecka, The Effect of Friction Stir Processing (FSP) on the Microstructure and Properties of AM60 Magnesium Alloy. Archives of Metallurgy and Materials **61**, 1209-1214 (2016).

[18] J. Liu, G. Li, D. Chen, Z. Chen, Effect of Cryogenic Treatment on Deformation Behavior of As-cast AZ91 Mg Alloy. Chinese J. Aeronaut. **25**, 931-936 (2012).

[19] S. Katoch, R. Sehgal, V. Singh, Study of the Effect of Deep Cryogenic Treatment on the Mechanical Properties of Hot Die Steel AISI-H13. i-manager's Journal on Material Science **4**, 9-18 (2016).

[20] B. Gassama, M.Ö. Öteyaka, Influence of cryogenic treatment on the corrosion of AZ91 and AM60 magnesium alloys in an isotonic solution. Mater. Test **61**, 1039-1044 (2019).

[21] M. Preciado, P.M. Bravo, J.M. Alegre, Effect of low temperature tempering prior cryogenic treatment on carburized steels. Journal of Materials Processing Technology **176**, 41-44 (2006).

[22] V. Bhavar, S. Khot, P. Kattire, M. Mehata, R. Singh, Effect of Deep Cryogenic Treatment on AISI H-13 Tool Steel. In: 28th ASM Heat Treating Society Conference, 28th ASM Heat Treating Society Conference, p. 383-389 (2015).

[23] D. Mohan Lal, S. Renganarayanan, A. Kalanidhi, Cryogenic treatment to augment wear resistance of tool and die steels. Cryogenics **41**, 149-155 (2001).

[24] T. Sonar, S. Lomte, C. Gogte, Cryogenic Treatment of Metal – A Review. Mater. Today-Proc. **5**, 25219-25228 (2018).

[25] F.H. Çakir, O.N. Çelik, Influence of Cryogenic Treatment on Microstructure and Mechanical Properties of Ti6Al4V Alloy. Journal of Materials Engineering and Performance **29**, 6974-6984 (2020).

[26] K.E. Lulay, K. Khan, D. Chaaya, The effect of cryogenic treatments on 7075 aluminum alloy. Journal of Materials Engineering and Performance **11**, 479-480 (2002).

[27] V. Franco Steier, E.S. Ashiuchi, L. Reißig, J.A. Araújo, Effect of a Deep Cryogenic Treatment on Wear and Microstructure of a 6101 Aluminum Alloy. Advances in Materials Science and Engineering **2016**, 1582490 (2016).

[28] M.Ö. Öteyaka, B. Karahisar, H.C. Öteyaka, The Impact of Solution Treatment Time (T6) and Deep Cryogenic Treatment on the Microstructure and Wear Performance of Magnesium Alloy AZ91. Journal of Materials Engineering and Performance **29**, 5995-6001 (2020).

[29] M. Vončina, M. Petrič, P. Mrvar, J. Medved, Thermodynamic characterization of solidification and defects that occur in Mg-alloy AM60. Journal of Mining and Metallurgy, Section B: Metallurgy **53**, 9-9 (2017).

[30] B. Kondori, R. Mahmudi, Effect of Ca additions on the microstructure, thermal stability and mechanical properties of a cast AM60 magnesium alloy. Mater. Sci. Eng. A **527**, 2014-2021 (2010).

[31] Q. Ma, H. El Kadiri, A.L. Oppedal, J.C. Baird, M.F. Horstemeyer, M. Cherkaoui, Twinning and double twinning upon compression of prismatic textures in an AM30 magnesium alloy. Scripta Materialia **64**, 813-816 (2011).

[32] H. Guo, S. Du, J. Lei, Y. Zhang, L. Hu, Influence of Twin Carbide Structure on Friction and Wear Properties of G95Cr18 Stainless Bearing Steel. Frontiers in Materials **6**, (2019).

[33] B. Mao, A. Siddaiah, X. Zhang, B. Li, P.L. Menezes, Y. Liao, The influence of surface pre-twinning on the friction and wear per-

formance of an AZ31B Mg alloy. Appl. Surf. Sci. **480**, 998-1007 (2019).

[34] A.A. Khaleghi, F. Akbaripanah, M. Sabbaghian, K. Máthis, P. Minárik, J. Veselý, M. El-Tahawy, J. Gubicza, Influence of high-pressure torsion on microstructure, hardness and shear strength of AM60 magnesium alloy. Mater. Sci. Eng. A **799**, 140158 (2021).

[35] M.Ö. Öteyaka, Influence of the addition of Ca and Sr on corrosion in aqueous solutions of magnesium alloys AZ And ZA. In, Laval University, p. 172 (2002).

[36] P. Bassani, E. Gariboldi, A. Tuissi, Calorimetric analysis of AM60 magnesium alloy. Journal of Thermal Analysis and Calorimetry **80**, 739-747 (2005).

[37] T. Oršulová, P. Palček, Changes in hardness of magnesium alloys due to precipitation hardening. Production Engineering Archives **18**, 46-49 (2018).

[38] C. Taltavull, B. Torres, A.J. López, J. Rams, Dry sliding wear behavior of AM60B magnesium alloy. Wear **301**, 615-625 (2013).

[39] A. Kumar, S. Kumar, N.K. Mukhopadhyay, A. Yadav, V. Kumar, J. Winczek, Effect of Variation of SiC Reinforcement on Wear Behaviour of AZ91 Alloy Composites. Materials **14**, (2021).

[40] E.E. Demirci, E. Arslan, K.V. Ezirmik, Ö. Baran, Y. Totik, İ. Efeoglu, Investigation of wear, corrosion and tribocorrosion properties of AZ91 Mg alloy coated by micro arc oxidation process in the different electrolyte solutions. Thin Solid Films **528**, 116-122 (2013).

[41] P. Metalnikov, G. Ben-Hamu, K.S. Shin, A. Eliezer, Effect of Ca Addition on Corrosion Behavior of Wrought AM60 Magnesium Alloy in Alkaline Solutions. Metals (2021).

[42] M.Ö. Öteyaka, E. Ghali, R. Tremblay, Corrosion Behaviour of AZ and ZA Magnesium Alloys in Alkaline Chloride Media. Int. J. Corr. **2012**, 452631 (2012).

[43] R.-C. Zeng, J. Zhang, W.-J. Huang, W. Dietzel, K.U. Kainer, C. Blawert, W. Ke, Review of studies on corrosion of magnesium alloys. T. Nonferr. Metal. Soc. **16**, s763-s771 (2006).